applied sciences

MDPI

Article

Organic Electrochemical Transistor Microplate for Real-Time Cell Culture Monitoring

Ota Salyk [1,*], Jan Víteček [2], Lukáš Omasta [1], Eva Šafaříková [2,3], Stanislav Stříteský [1], Martin Vala [1] and Martin Weiter [1]

1 Materials Research Centre, Faculty of Chemistry, Brno University of Technology, Purkyňova 118, 61200 Brno, Czech Republic; xcomastal@fch.vut.cz (L.O.); xcstritesky@fch.vutbr.cz (S.S.); vala@fch.vutbr.cz (M.V.); weiter@fch.vutbr.cz (M.W.)

2 Institute of Biophysics AS CR, Královopolská 135, 61265 Brno, Czech Republic; jan.vitecek@ibp.cz (J.V.); safarikova.eva@ibp.cz (E.Š.)

3 Department of Experimental Biology, Faculty of Science, Masaryk University, University Campus Bohunice, Kamenice 5, 62500 Brno, Czech Republic

* Correspondence: salyk@fch.vut.cz; Tel.: +420-541-149-414

Received: 20 July 2017; Accepted: 18 September 2017; Published: 27 September 2017

Featured Application: The intended application is in drug toxicity testing on cardiomyocytes, replacing experimental animals and investigating the signal of electrogenic cells.

Abstract: Human cell cultures provide a potentially powerful means for pharmacological and toxicological research. A microplate with a multielectrode array of 96 organic electrochemical transistors (OECTs) based on the semiconductive polymer poly(3,4-ethylenedioxythio-phene):poly (styrene sulfonic acid) PEDOT:PSS was developed and fabricated by the screen printing method. It consists of a microplate of a 12 × 8 chimney–well array with transistors on the bottom. The OECT is circular with a channel of 1.5 mm^2 in the centre surrounded by the circular gate electrode. The device is designed for electrogenic cell monitoring. Simulations with the electrolyte revealed good electrical characteristics and indicated the setup information of the experimental conditions. A transconductance of g = 1.4 mS was achieved in the wide range of gate voltages $V_{gs} = \pm 0.4$ V when the drain potential $V_{ds} = -0.735$ V was set and the long term relaxation was compensated for. The time constant 0.15 s limited by the channel-electrolyte charge electrical double layer (EDL) capacitance was measured. The device was tested on a 3T3 fibroblast cell culture and the sudden environmental changes were recorded. The living cells can be observed on the channel of the OECT and during electrical stimulation by gate voltage, as well as during the source current response.

Keywords: OECT; screen printing; organic electrochemical transistor; PEDOT:PSS; microplate; multi-electrode array; cell culture

1. Introduction

The current trend in toxicology and pharmacology focuses on the substitution of experimental animals with in-vitro cell-based systems. This requires the introduction of approaches for the real-time determination of cell physiology. Electrochemical sensors can serve this purpose. Furthermore, the use of organic semiconductors allows for the production of disposable sensors at a low cost. Poly(3,4-ethylenedioxythio-phene) mixed with poly(styrene sulfonic acid)—(PEDOT:PSS) has become the most convenient material among organic semiconductors for bioelectronic applications because of its high conductivity and biocompatibility. The theoretical model of an Organic Electrochemical Transistor (OECT) based on PEDOT:PSS, which was published in 2007 [1], has enabled the optimization and further development in bioelectronic applications. The model describes both the steady state and

transient response of the ionic and hole channel current on gate voltage. An amended model taking into account nonlinearities in charge carrier mobility and optical absorption variation was presented in 2015 [2]. The functional improvement consists of geometry optimization in order to maximize the OECT transconductance [3], working point setting to zero gate voltage [4], miniaturizing for one cell monitoring down to a channel length of 6 µm, and a fast response down to a 100 µs time constant [5].

The OECT architecture can be planar, when the PEDOT:PSS channel and gate are deposited by spin coating, inkjet printing [6], and screen printing methods, as well as using the microlithographic technique. The gate electrode can either be situated in the electrolyte bulk above the channel using gold or Ag/AgCl wire as a biocompatible material or be deposited as a part of a planar electrode system on a substrate.

Several reviews have been dedicated to both the investigation of general properties [7] and biological applications [8–10]. According to a recent review [11], biological applications can target several specific goals: ion sensors, enzymatic sensors, and immunosensors-nucleotide sensors, coupled with entire cells for electrophysiology, the integration of OECTs with nonelectrogenic cells, OECT for stimulations, and the recording of electrogenic cells. These have already been tested in human biology and experimental medicine either for diagnostics or treatment [12]. Others have combined optical and electrical sensing for the investigation of epithelial cells [13]. The OECT channel coverage by cells was evaluated by the time response of the channel current on the gate rectangular pulse. Campana et al. [14] used OECT in a resorbable bioscaffold from poly(L-lactide-*co*-glycolide) for cardiographic recording.

Wang et al. (2013) [15] investigated the influence of antiarrhythmic drugs on cardiomyocytes by the simultaneous monitoring of the impedance signal of a cell set in a biosensor plate well containing a gold electrode system. Later, Yao et al. (2015) [16] used a similar well plate equipped with OECTs for signal amplification. Leleux et al. (2015) [17] successfully used OECTs in recording the cardiac rhythm, eye movement, and brain activity of a human volunteer. Wan et al. (2015) [18] reported the fabrication of a 3D biocompatible macroporous PEDOT:PSS scaffold supporting the fibroblast culture and the ability to electrically monitor various cell functions. They observed a positive potential influence on cell adherence enhancement, resulting in a higher relative number of adhered cells on an oxidized (+1 V) surface. Hempel et al. (2016) [19] developed an electrophysiological biosensor for investigating the electrogenic activity of cardiac cells by means of a multi-electrode array.

The goal of this study is to investigate the possibility of OECTs based on the application of PEDOT:PSS and fabrication of a planar all-screen-printed 12 × 8 microplate array of transistors.

2. Materials and Methods

The device (see Figure 1) was constructed on a 96-well polystyrene microplate (chimney-well, no bottom) from Greiner Bio-One (GmbH Frickenhausen, Frickenhausen, Germany), for the automated analysis of a multitude of substances. We provided the bottom with the all-printed 12 × 8 array of Organic Electrochemical Transistors (OECT) based on the Poly(3,4-ethylenedioxythiophene) polystyrene sulfonate (PEDOT:PSS) polymer (Clevios™ S V3, Heraeus Holding GmbH, Hanau, Germany). The screen-printing method was used. Printed organic electronic technology has generated the possibility of printing biosensor patterns on biocompatible polymer foils of PET (Poly(Ethylene Terephthalate)) or PEN (Poly(Ethylene 2,6-Naphthalate) (both Goodfellow Cambridge Ltd., Huntingdon, UK), the latter of which enables processing at a temperature of up to 170 °C. The bottom substrate was a 0.25 mm thick PEN foil due to better thermal stability during the subsequent annealing processing of the prints. The first printed pattern (screen mesh count 77 threads/cm) of silver paste CB115v2 (©DuPont) Photopolymer and Electronic Materials, Wilmington, DE, USA) creates the contact and conductive field and the paths that are 0.18 mm in width (see Figure 1d). The foil with the silver pattern was then annealed at 120 °C for fixation.

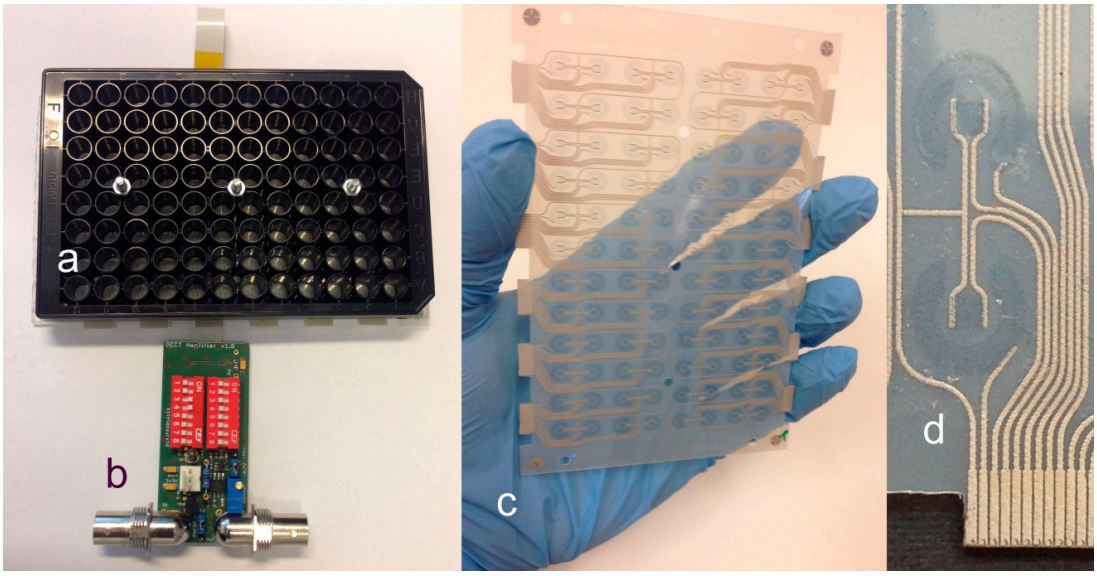

Figure 1. Encapsulated organic electrochemical transistor (OECT) 96 well microplate for electrogenic cell cultivation and investigation (**a**) with a power source-signal amplifier and current/voltage converter (**b**), foil with functional printed patterns of all OECTs in a 12 × 8 array (**c**), and a detail of a couple of OECTs with a poly(3,4-ethylenedioxythio-phene) :poly(styrene sulfonic acid)—PEDOT:PSS printed channel and gate electrode (**d**).

The second pattern of PEDOT:PSS paste Clevios™ S V3 (screen mesh count 140 threads/cm) created a functional OECT gate and channel. The paste was first stirred intensively before printing in order to obtain a lower viscosity and better homogeneity of the resulting film. An ARG2 rheometer (TA Instruments, New Castle, DE, USA) was used for viscosity testing at various shear rates and always at 25 °C, but only the initial low rate viscosity is presented. The paste of gel consistency exhibits thixotropy. The static viscosity (at shear rates of 0.1/s) falls from the initial value above 1000 Pa·s down to ultimately 14 Pa·s after five days of stirring in a magnetic mixer at a laboratory temperature of 25 °C. The stirring temperature of 90 °C shortened the time needed to 24 h. The viscosity did not then decrease further by further stirring. After the stirring was ceased, the viscosity returned to the initial value, with 100 Pa·s measured after about 1 h, illustrating that the printing has to be performed within a few minutes, before the consistency of the paste returns back to the initial gel state. The channel dimensions are 1.5 × 1.5 mm width × length and the gate is created by printing a ring broken on one side for source and drain contacting. The silver conductive paste and the polymer patterns were annealed using a hot plate at 150 °C for 15 and 30 min, respectively, in air for the film's stabilization and adhesion improvement.

The stirring effect slightly decreased the final thickness by an average of 20% from 250 nm to 200 nm. It also improved the thickness homogeneity in roughness from 25 nm to 18 nm and waviness from 25 nm to 10 nm, measured by a DetakXT profilemeter (Bruker, Billerica, MA, USA) (see Figures S1 and S2). Additionally, the sheet resistance decreased significantly from about 800 Ω/□ to 400 Ω/□. It is considered that intensive stirring acts similarly to alcohol treatment. Furthermore, the core–shell molecular structure changes in a linear fashion as was already reported in [20] and the process is reversible. This can also explain the resistance, roughness, and waviness reduction. The improvement in homogeneity can be observed by an optical microscope according to the round interference fringes on the PEDOT:PSS layer (see Figure S3).

The system is masked and sealed by the third pattern of the Sylgard® 184 (Dow Corning, Midland, MI, USA) silicone elastomer (mesh count 120 threads/cm), which insulates the silver conducting paths from the electrolyte environment and also prevents the tested biomaterial from coming into contact with the non-biocompatible parts and layers of the printed device. The silicone elastomer pattern was

left to polymerize at 60 °C for at least 8 h before further manipulation. The following screen print provided a layer with a thickness of 12 µm (see Figure S4). Other parts and materials were tested for biocompatibility [21]. A coating to increase biocompatibility was produced with murine collagen type IV (BD Biosciences, cat. No. 354233) at 10 µg·cm^{-2} according to the manufacturer's instructions.

Patterning and microplate completing followed. The OECT's channel visible in Figure 1d, created by a screen-printed rectangular PEDOT:PSS layer on PEN foil, is surrounded by a planar circular gate electrode with a 6 mm outer diameter. The rotary symmetry is expected to improve the field distribution. The electrodes are contacted by printed silver conductors of a 0.2 mm width. The printed transparent silicone layer covers the surface of the sensing array with the exception of the functional PEDOT:PSS interfacing to the biomaterial and physiological solution. The exposed channel area is of a length of L = 1 mm and a width of W = 1.5 mm, the thickness of the PEDOT:PSS layer was 250 nm on average, and the typical resistance of the channel was 500–700 Ω. The foil was firmly fixed to the polystyrene microplate and bolted down from the bottom by means of a Plexiglas® plate in order to enable easier handling and transparency needed for microscope observations.

The electrical circuitry designed for OECT testing in schematic form is depicted in Figure 2. The contact array on the microplate foil was contacted by 18-pin Molex connectors and 18-wire ribbon conductors so that eight OECTs were connected by a single connector and individual OECTs can be selected from the array by a proper couple of microswitches. The gate potential V_{gs} is set from the outer source in a range from −0.8 V to 0.8 V with respect to preventing redox reactions on electrodes and a source drain voltage V_{ds} down to −0.725 V can be set. The source current I_s was converted to voltage in an I/V converter and recorded by a scope after further amplification. The offset I_s at a stable working point can be compensated for by setting the corresponding opposite current at the input of the operating amplifier. The zero Analog OUT voltage can be set for an input voltage of V_{gs} = 0 V with the aid of a R_{offset} resistor/potentiometer. The feedback resistor R_{sense} = 1 kΩ gives a conversion of 1 mA/1 V. Further amplification is enabled by switching the output jumper.

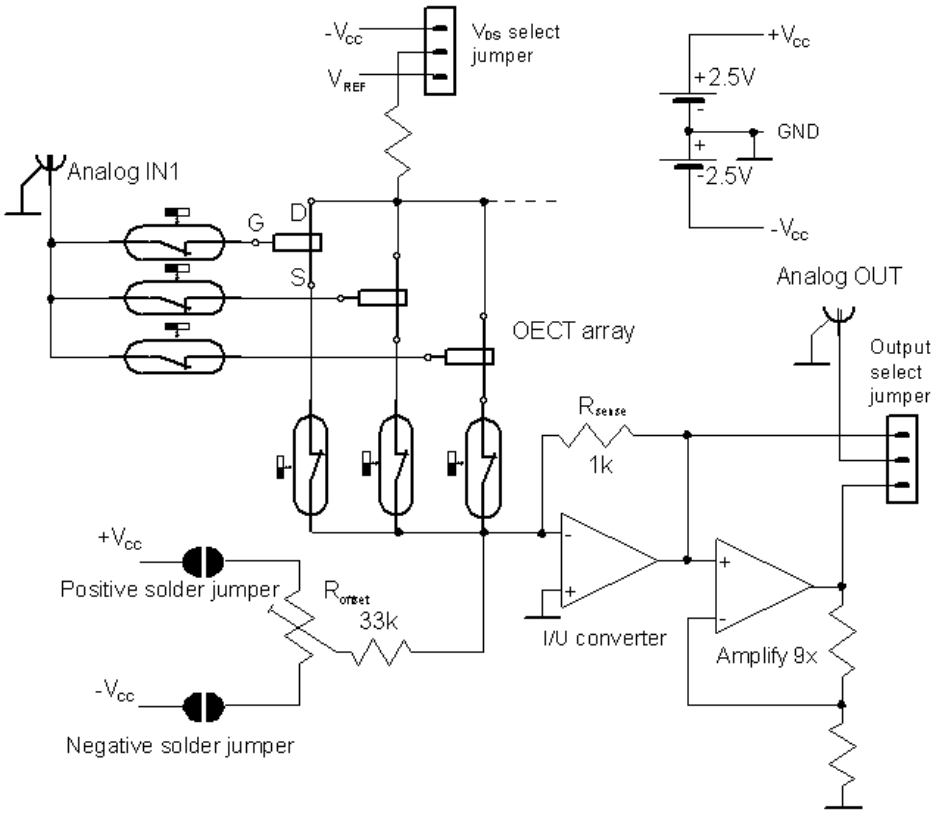

Figure 2. The principle of selecting and testing a single OECT from the 96 OECTs array.

OECTs are a promising tool for measuring the electrical pulsation of electrogenic cells. Their electric field can penetrate through the cell membrane into the surrounding phosphate-buffered saline (PBS) electrolyte and the channel electrode. Their pulsing potential can be simulated by the modulation of the gate voltage V_{gs}. Besides the gate voltage, the size of the channel area and electrode arrangement determine the sensitivity and signal to noise ratio. The field strength at the channel vicinity determines the effective ion drift in and out of the channel and consequently the channel conductance. The small channel area facing the electrolyte compared with the gate electrode area enhances the field and lowers the electrical double layer (EDL) capacitance per unit area at the PEDOT:PSS, which is responsible for the device speed. The capacitance of the electrode in a physiological solution of phosphate-buffered saline (PBS) based on a 0.15 M solution of NaCl was estimated at $C = 0.2$ μF·mm^{-2}. Together with the electrolyte conductance $G = 1$ μS, the time constant $\tau = C/G = 0.2$ s was anticipated. The capacitance of the much larger gate charge EDL can be neglected due to its serial combination with the channel capacitance. The speed of the OECT device is limited by the capacitance of the gate circuit. It is controlled by the effective capacitance of the channel. The label 'effective' here takes into account that the potential at the channel is not uniform but distributed non-linearly along its length from the source to the drain electrode (from 0 to −0.725 V in our case). It can be, to some degree, considered a consequence of the channel aspect ratio. Moreover, the geometry of the entire system including the gate electrode and electrolyte can influence the channel potential distribution. Contrary to the majority of authors, we use the planar arrangement of the electrodes for an easy optical and camera investigation. The computer modelling of the system has still not been satisfactorily solved.

The testing and gate offset voltage, as well the modulation (simulating the cardiomyocyte pulsing), were delivered from a function generator to the Analog IN input. An OECT was selected by a couple of switches. The drain is supplied by a negative voltage down to $V_{ds} = -0.735$ V. This value is a factory setting and it represents a compromise between the requirement of a safety voltage against electrode redox reactions in the event of a positive $V_{gs} > 0$ V gate voltage and the requirement of high amplification (transconductance). Its fixed value enables comparing the amplification of our various OECT devices at any point in time. The source is connected to a virtual zero input of the I/V converter. The amplified signal was recorded by a digital memory scope. The offset of the stable channel current was compensated for by a potentiometer R_{offset} so the Analog OUT DC signal component could be eliminated.

Mouse 3T3 fibroblasts (cat. No. CRL-1658, ATCC, Manassas, VA, USA) were routinely grown in Dulbecco modified Eagle medium, high glucose supplemented with 10% fetal calf serum, 100 U/mL penicillin, and 0.1 mg/mL streptomycin (all from Gibco, Gaithersburg, MD, USA) in standard 100 mm cell culture dishes (cat. No. 93100, TPP, Trasadingen Switzerland), as described previously [22]. The inocula for experiments ranged from 8300 to 28,000 cells per 1 cm^2. Viability was routinely checked by means of a cytometer (CASY, Roche Diagnostics Ltd., Rotkreuz, Switzerland). Cells were grown in sensors for 48 h.

To provide proof of sensor function, cells grown within the experiment were washed with physiological buffered saline two times and 200 μL of 0.25% trypsin (cat. No. R001100, Gibco, Gaithersburg, MD, USA) was added. Together with the addition of trypsin, video recording was started.

3. Results and Discussion

The first experiment tested the OECT parameters as the transfer characteristics and the derived transconductance g. The fix drain potential was set to $V_{ds} = -0.735$ V and the output source current was measured continuously at the triangular symmetric gate voltage V_{gs} in a range of 0.2 to −0.8V. The results can be found in Figure 3. As can be seen from the figure, due to relaxations, the transfer characteristics and transconductance $g = \mathrm{d}I_s/\mathrm{d}V_{gs}$ included are strongly dependent on the sweep rate of the testing gate voltage V_{gs} and its direction. The sharp transconductance maximum was observed first by Rivnay et al. [4]. Its position on the V_{gs} axis depends on the channel geometry, but no sweep

rate influence was reported. The transfer characteristics in our case show significant hysteresis. In the case of a short period of about T = 1 s, the EDL capacitance charging delays the output current I_s, so the hysteresis is oriented counter-clockwise. In the case of a long period of T = 20 s, slow relaxations of the polymer network in the channel, reducing the output current I_s, dominate so that the hysteresis is oriented clockwise. In the case of a medium period of T = 5 s, both effects are compensated.

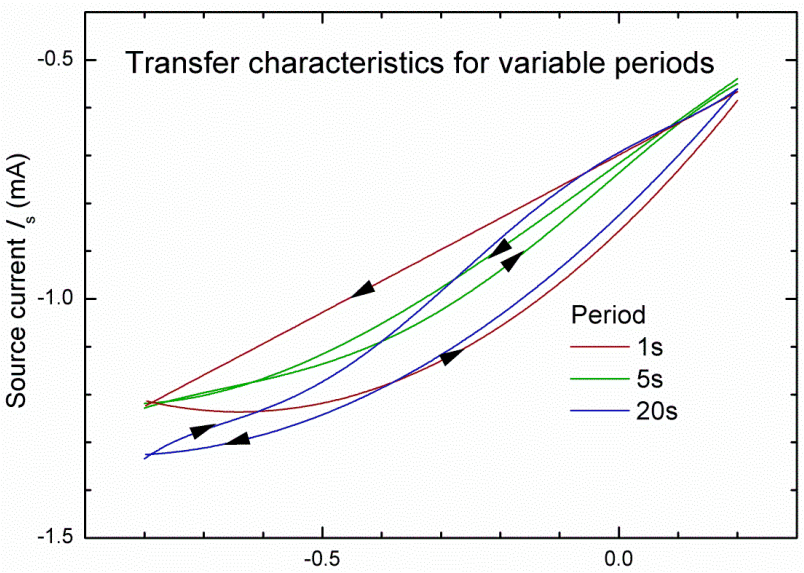

Figure 3. Transfer characteristics measured at the triangular gate periodic voltage at various periods.

A second experiment, investigating the response of an OECT's channel current on a simulated signal of electrogenic cells, was carried out (Figure 4). The standard PBS solution was used as an electrolyte. In looking for the optimum working point of the OECT with the highest transconductance, the gate voltage V_{gs} from the function generator was modulated by rectangular pulses of 10 mV_{pp} over a 5 s period. This was superposited on the offset voltage, as can be seen in Figure 4. While the response on the offset setting showed negative relaxation with a time constant of approximately 25 s, the amplification of the pulsing signal did not change significantly according to the offset. This means that the transconductance remains constant across a wide range of gate offsets, in our case a transconductance of g = 0.01 mA/0.01 V = 1 mS deduced from the plot. However, this value is limited by the frequency band pass f = (0.2–8.0) Hz corresponding to the time constants of the gate circuit and slow relaxation processes. The measured time constant τ = 0.12 s achieved by the simple exponential fitting corresponds to charging–discharging the channel EDL capacitance of C = 0.1 µF and the entire gate circuit resistance of R = 1.2 MΩ. The potential on the capacitance varies and it also controls the ion doping–dedoping process. The measured circuit current, charging the gate, achieved 1 µA in accordance with the circuit resistance. It is theoretically possible to lower the time constant by decreasing the channel area and hence its capacitance or by decreasing the gate-channel distance and hence its resistance. The resistivity of the electrolyte is determined by its physiological function and so it cannot be variated. The speed of the device is then limited by the screen-printing resolution. The lithographic technique enables the development of much smaller dimensions and quicker devices. This is necessary for recording the shape of the electrogenic cell (cardiomyocyte) signal.

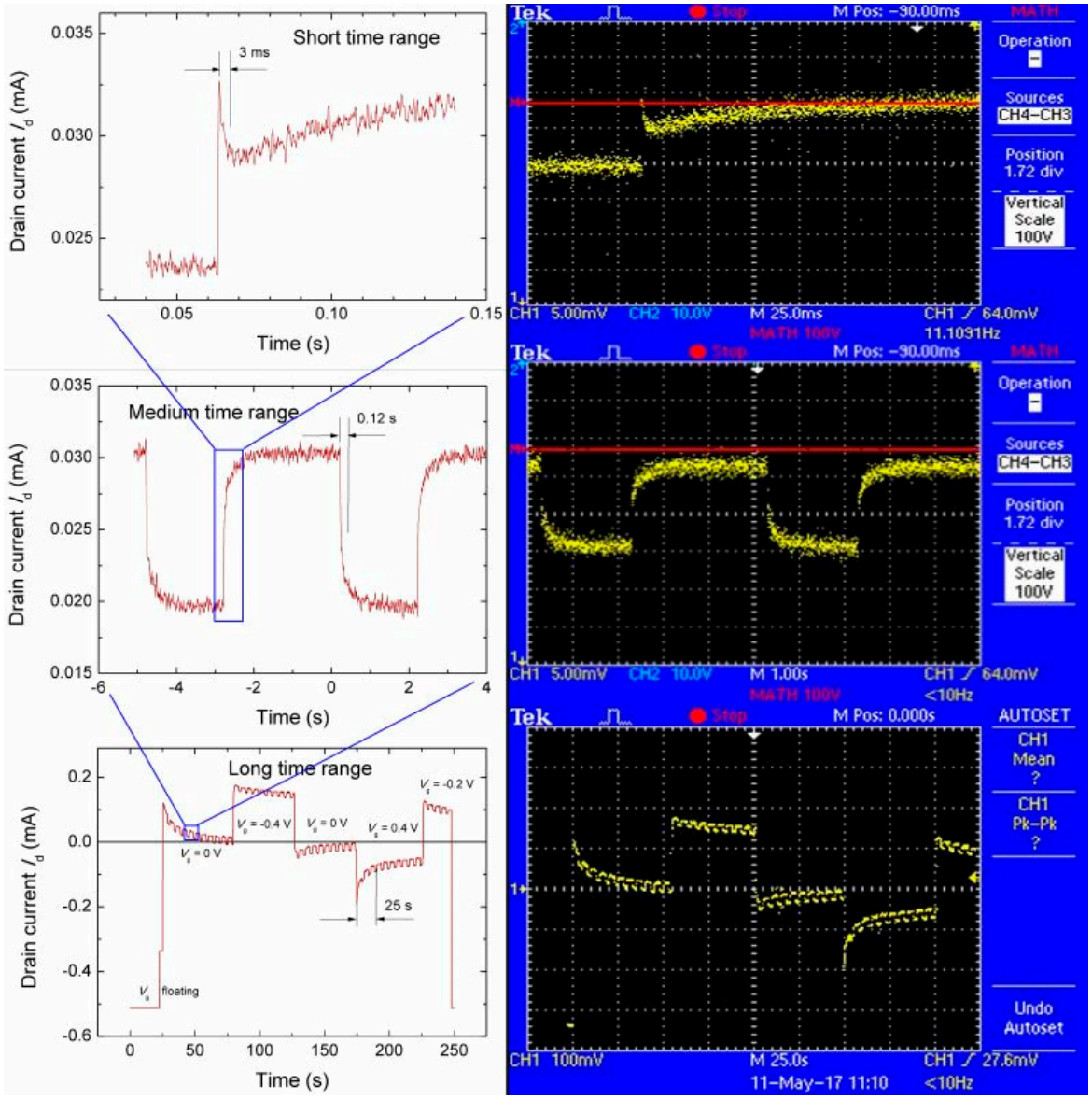

Figure 4. Response of output voltage of the preamplifier - I/V converter (calibrated in drain current units) on the gate input voltage at $V_{ds} = -0.735$ V and variable gate voltage V_{gs} modulated by rectangular pulses of voltage 10 mV_{pp} and a 5 s period.

Using a short time range display, we found one further time constant, namely 3 ms caused by hole extraction and injection into the channel [1]. This might play a more significant role in a smaller channel area with a lower capacitance and time constant.

The faster rectangular modulation, applied to the V_{gs} simulating a signal of electrogenic cells (cardiomyocytes), lent importance to the measurement. A period of 5 s was set in order to get the source current I_s to a sufficiently steady state (Figure 4, medium time range) for the deduction of the time constant τ of the gate circuit. The medium current response is almost not influenced by material relaxation. The ΔI_s response on the modulation represents a consequence controlled by charging and discharging the EDL capacitance at the electrolyte—PEDOT:PSS interface.

At the moment of the gate pulse edge, a short source current I_s spike appears with an exponential decay that is constant at about 3 ms. This is considered the effect of the hole extraction/injection process in the PEDOT:PSS channel, as was already described by Bernards and Malliaras [1].

The aging of the OECT structure under the voltage load described above was performed over a period of 28 h (see Figure S5). A gradual, approximately 25% decrease of I_s and the transconductance g was recorded.

The biocompatibility of the sensor was tested by 3T3 fibroblasts. These cells were able to grow within sensors to the same extent as in the control (standard cell culture plastics, not shown). The viability was comparable to the control and it typically reached 90–95%. This indicated that a high level of biocompatibility was reached. Indeed, cells were able to form a confluent layer within 48 h (Figure 5A).

A proof-of-concept experiment for the sensor function was carried out. Due to extensive ion exchange, the cells growing at the transistor channel modulate the current within it; hence the removal of cells will result in changes to the channel current. Thus, the confluent layer of cells within the sensor was treated with trypsine, an approach to detach cells from their support [9]. Indeed, the absolute value of the current decreased in parallel with the trypsine-mediated detachment of cells (Figure 5B, see video S1). Finally the function of the sensor was verified by means of a spike of KCl (Lachema, Brno, Czech Republic), which resulted in a major dropdown of the absolute current value. The main idea of the final proof of concept experiment with cells was to demonstrate that the sensor can host the living cells efficiently and an electrogenic event related to cell physiology could be recorded.

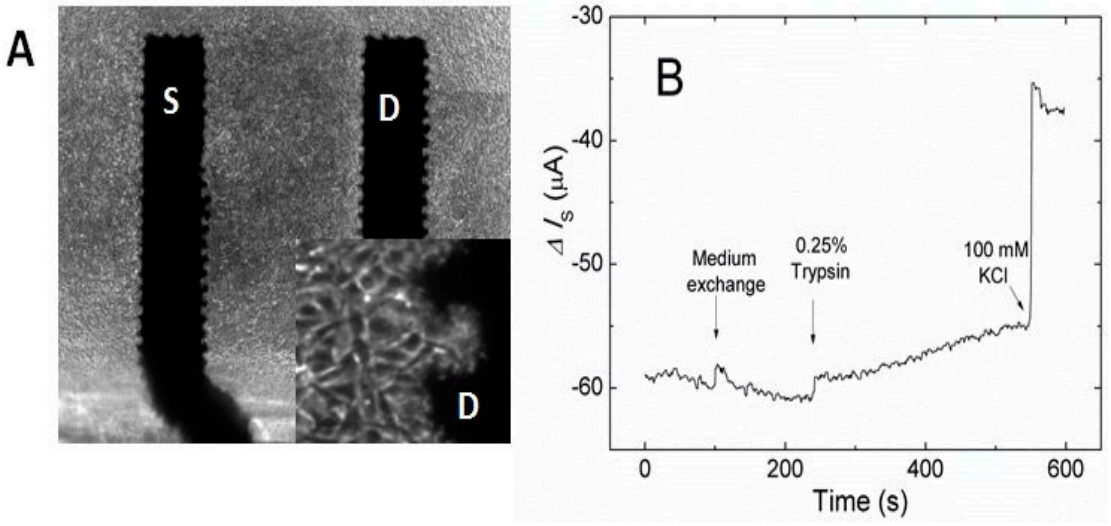

Figure 5. Electrochemical transistor with confluent layer of 3T3 fibroblasts: S—source, D—drain (**A**). The electrical response to cell release due to trypsin. 100 mM KCl spike served as a positive control of transistor function (**B**). Typical results out of three biological replicates are shown.

4. Conclusions

An all-screen-printed 12 × 8 array of OECTs for cell culture electrical response monitoring was developed. These PEDOT:PSS-based OECTs showed long-term relaxation with problematically defined gain and transconductance due to long-term material relaxation in the electrolyte and the electrical field environment. On the other hand, electrogenic cells produce a periodic short-term gate potential event up to 5 s in range. Such a corresponding signal has uniform amplification across a wide range of gate potential offsets (±0.4 V). This is demonstrated by means of a simulation, where the stable gate offset potential was modulated by a 0.2 Hz, 10 mV_{pp} rectangular signal. The resulting source current response ΔI_s was 10 μA and the corresponding achieved transconductance was 1 mS. The upper frequency limit 8 Hz was deduced from the OECT gate circuit time constant of 0.12 Hz. The measuring circuit was equipped with a current source for the suppression of the stable offset.

Further improvement of the device speed can be achieved by decreasing the OECT dimensions by shortening the gate-channel distance and minimizing the EDL capacitance by reducing the

channel area below the resolution limits of screen printing, which must therefore be replaced by a higher-resolution technology.

The usefulness of the device for working with biological material was demonstrated using a 3T3 fibroblast. Indeed, the device showed high biocompatibility and a good response to the trypsin-mediated detachment of cells. Therefore, the developed device is a good starting point for the efficient monitoring of cells in biological applications.

Supplementary Materials: The following are available online at http://www.mdpi.com/2076-3417/7/10/998/s1, Figure S1: Profile of screen printed PEDOT:PSS layer Clevios SV3. The comparison of the profile of the resulting layer (A) using non stirred (as obtained) and (B) stirred paste. (The record from the profilemeter DetakXT (Bruker)), Figure S2: Profile of screen printed PEDOT:PSS layer Clevios SV3. The comparison of the profile of the resulting layer (A) using non–stirred (as obtained) and (B) stirred paste. (The record from the profilemeter DetakXT (Bruker)), Figure S3: Screen printed layers with channel resistances of stirred PEDOT:PSS paste Clevios SV3 (A) non stirred, (B) stirred 30 min. (C) stirred 2 hours, (D) stirred 3 days. Figure S4: Thickness and roughness of screen printed PEDOT:PSS and silicone layers, Figure S5: PEDOT:PSS OECT degradation at $V_{ds} = -0{,}735$ V and $V_{gs} = 0$V in PBS solution, Video S1: 3T3 fibroblast detachment.

Acknowledgments: This work was supported by the Czech Science Foundation, Czech Republic via Project shear 13-29358S; research infrastructure was supported via the Materials Research Centre at FCH BUT–Sustainability and Development, REG LO1211, with financial support from the National Programme for Sustainability I (Ministry of Education, Youth and Sports).

Author Contributions: Ota Salyk designed the microplate with a multielectrode array of 96 organic electrochemical transistors (OECTs), tested the functionality in simulated conditions, and wrote the paper; Jan Víteček and Eva Šafaříková cultivated the cell culture and participated on the biological site of their testing; Lukáš Omasta developed the technology of PEDOT:PSS screen printing; Stanislav Stříteský developed the measuring system based on National Instruments units and LabView® software and performed the electrical measurements on living cells; Martin Vala contributed in the field of theoretical insight and explanation of the OECT behaviour; Martin Weiter, the project manager and investigator, conceived the idea of the experiment.

Conflicts of Interest: The authors declare no conflict of interest.

References

1. Bernards, D.A.; Malliaras, G.G. Steady-state and transient behavior of organic electrochemical transistors. *Adv. Funct. Mater.* **2007**, *17*, 3538–3544. [CrossRef]
2. Friedlein, J.T.; Shaheen, S.E.; Malliaras, G.G.; McLeod, R.R. Optical Measurements Revealing Nonuniform Hole Mobility in Organic Electrochemical Transistors. *Adv. Electron. Mater.* **2015**, *1*. [CrossRef]
3. Khodagholy, D.; Rivnay, J.; Sessolo, M.; Gurfinkel, M.; Leleux, P.; Jimison, L.H.; Stavrinidou, E.; Herve, T.; Sanaur, S.; Owens, R.M.; et al. High transconductance organic electrochemical transistors. *Nat. Commun.* **2013**, *4*, 2133. [CrossRef] [PubMed]
4. Rivnay, J.; Leleux, P.; Sessolo, M.; Khodagholy, D.; Herve, T.; Fiocchi, M.; Malliaras, G.G. Organic Electrochemical Transistors with Maximum Transconductance at Zero Gate Bias. *Adv. Mater.* **2013**, *25*, 7010–7014. [CrossRef] [PubMed]
5. Khodagholy, D.; Gurfinkel, M.; Stavrinidou, E.; Leleux, P.; Herve, T.; Sanaur, S.; Malliaras, G.G. High speed and high density organic electrochemical transistor arrays. *Appl. Phys. Lett.* **2011**, *99*, 227. [CrossRef]
6. Basirico, L.; Cosseddu, P.; Scida, A.; Fraboni, B.; Malliaras, G.G.; Bonfiglio, A. Electrical characteristics of ink-jet printed, all-polymer electrochemical transistors. *Org. Electron.* **2012**, *13*, 244–248. [CrossRef]
7. Kergoat, L.; Piro, B.; Berggren, M.; Horowitz, G.; Pham, M.C. Advances in organic transistor-based biosensors: From organic electrochemical transistors to electrolyte-gated organic field-effect transistors. *Anal. Bioanal. Chem.* **2012**, *402*, 1813–1826. [CrossRef] [PubMed]
8. Owens, R.M.; Malliaras, G.G. Organic Electronics at the Interface with Biology. *Mrs Bull.* **2010**, *35*, 449–456. [CrossRef]
9. Lin, P.; Yan, F.; Yu, J.J.; Chan, H.L.W.; Yang, M. The Application of Organic Electrochemical Transistors in Cell-Based Biosensors. *Adv. Mater.* **2010**, *22*, 3655. [CrossRef] [PubMed]
10. Liao, C.Z.; Yan, F. Organic Semiconductors in Organic Thin-Film Transistor-Based Chemical and Biological Sensors. *Polym. Rev.* **2013**, *53*, 352–406. [CrossRef]
11. Strakosas, X.; Bongo, M.; Owens, R.M. The organic electrochemical transistor for biological applications. *J. Appl. Polym. Sci.* **2015**, *132*. [CrossRef]

12. Rivnay, J.; Owens, R.M.; Malliaras, G.G. The Rise of Organic Bioelectronics. *Chem. Mater.* **2014**, *26*, 679–685. [CrossRef]
13. Ramuz, M.; Hama, A.; Huerta, M.; Rivnay, J.; Leleux, P.; Owens, R.M. Combined Optical and Electronic Sensing of Epithelial Cells Using Planar Organic Transistors. *Adv. Mater.* **2014**, *26*, 7083–7090. [CrossRef] [PubMed]
14. Campana, A.; Cramer, T.; Simon, D.T.; Berggren, M.; Biscarini, F. Electrocardiographic Recording with Conformable Organic Electrochemical Transistor Fabricated on Resorbable Bioscaffold. *Adv. Mater.* **2014**, *26*, 3874–3878. [CrossRef] [PubMed]
15. Wang, T.X.; Hu, N.; Cao, J.Y.; Wu, J.Y.; Su, K.Q.; Wang, P. A cardiomyocyte-based biosensor for antiarrhythmic drug evaluation by simultaneously monitoring cell growth and beating. *Biosens. Bioelectron.* **2013**, *49*, 9–13. [CrossRef] [PubMed]
16. Yao, C.; Li, Q.; Guo, J.; Yan, F.; Hsing, I.M. Rigid and Flexible Organic Electrochemical Transistor Arrays for Monitoring Action Potentials from Electrogenic Cells. *Adv. Healthc. Mater.* **2015**, *4*, 528–533. [CrossRef] [PubMed]
17. Leleux, P.; Rivnay, J.; Lonjaret, T.; Badier, J.M.; Benar, C.; Herve, T.; Chauvel, P.; Malliaras, G.G. Organic Electrochemical Transistors for Clinical Applications. *Adv. Healthc. Mater.* **2015**, *4*, 142. [CrossRef] [PubMed]
18. Wan, A.M.-D.; Inal, S.; Williams, T.; Wang, K.; Leleux, P.; Estevez, L.; Giannelis, E.P.; Fischbach, C.; Malliaras, G.G.; Gourdon, D. 3D conducting polymer platforms for electrical control of protein conformation and cellular functions. *J. Mater. Chem. B* **2015**, *3*, 5040–5048. [CrossRef] [PubMed]
19. Hempel, F.; Law, J.K.-Y.; Nguyen, T.C.; Munief, W.; Lu, X.; Pachauri, V.; Susloparova, A.; Vu, X.T.; Ingebrandt, S. PEDOT:PSS organic electrochemical transistor arrays for extracellular electrophysiological sensing of cardiac cells. *Biosens. Bioelectron.* **2017**, *93*, 132–178. [CrossRef] [PubMed]
20. Alemu, D.; Wei, H.Y.; Ho, K.C.; Chu, C.W. Highly conductive PEDOT:PSS electrode by simple film treatment with methanol for ITO-free polymer solar cells. *Energy Environ. Sci.* **2012**, *5*, 9662–9671. [CrossRef]
21. Šafaříková, E.; Švihálková Šindlerová, L.; Stříteský, S.; Kubala, L.; Vala, M.; Weiter, M.; Víteček, J. Towards highly biocompatible organic semiconductors iterfaces for bioelectronic devices. *Sens. Actuators B Chem.* (submitted).
22. Vistejnova, L.; Dvorakova, J.; Hasova, M.; Muthny, T.; Velebny, V.; Soucek, K.; Kubala, L. The comparison of impedance-based method of cell proliferation monitoring with commonly used metabolic-based techniques. *Neuroendocrinol. Lett.* **2009**, *30*, 121–127.